Journal of
Synchrotron Radiation

ISSN 0909-0495

Received 5 April 2005
Accepted 18 August 2005

Highly time-resolved correlation measurement between laser and synchrotron radiation pulses without synchronization control

Yoshihiro Takagi,[a]* Makoto Nakano,[a] Kazuki Arikawa,[a] Kiyoshi Ishikawa,[a] Sho Amano,[b] Shuji Miyamoto[b] and Takayasu Mochizuki[b]

[a]Department of Materials Science, Graduate School of Materials Science, University of Hyogo, 3-2-1 Kohto, Kamigouri-Cho, Hyogo 678-1297, Japan, and [b]Laboratory of Advanced Science and Technology for Industry, University of Hyogo, 3-1-2 Kohto, Kamigouri-Cho, Hyogo 678-1205, Japan. E-mail: takagi@sci.u-hyogo.ac.jp

A mode-locked laser has been introduced in combination with synchrotron radiation to establish a versatile technique for highly time-resolved correlation measurements utilizing the short-pulse and high-pulse frequency characteristics of both photon sources. Successive pulse timing delay detected by nonlinear optical mixing between the two sources yields a cross-correlation profile capable of accurate measurement of the picosecond pulse profile of the synchrotron radiation without any synchronization control. Although the experiment was performed in the visible spectral domain, the present technique opens up a methodology for time-resolved spectroscopy in femtosecond and higher-energy domains by introducing a suitable nonlinear process that informs of the pulse coincidence between the two radiation sources.

Keywords: nonlinear optical mixing; sum-frequency generation; phase matching; optical klystrons; ultrafast; synchronization; sampling.

1. Introduction

Owing to recent progress in the use of ultrashort pulsed radiation from lasers and electron synchrotron storage rings (*e.g.* Rulliere, 2003; Wille, 1991), a growing number of time-resolved studies on ultrafast phenomena following impulsive excitation by the combined use of these radiation sources are being reported. The development of versatile methodology for highly time-resolved measurements is therefore a subject of practical interest. The primary requirement for realizing well controlled timing between two photon sources is to synchronize them, and indeed much effort has been made since the early days of the development of synchrotron storage rings (Meyer *et al.*, 1987; Mitani *et al.*, 1989; Lacoursiere *et al.*, 1994; Gatzke *et al.*, 1995, 1998; Winter *et al.*, 1998; Tanaka *et al.*, 2000). For construction of rigid electronic synchronization, the laser should be kept in a very stable mode-locked operation, including fine and fast mechanical control of cavity length to compensate for the fluctuation in pulse frequency. Here we propose an alternative approach, to carry out time-resolved synchrotron radiation and laser measurement avoiding exact synchronization, so that the instrumentation for the feedback system is omitted and the laser setting is greatly simplified. Ultrafast lasers generate highly repetitive pulses with frequencies of several tens to hundreds of megahertz and the synchrotron radiation pulses can be in the overlapped range depending on the electron bunch operation. Such high-frequency periodic pulse characteristics in both photon sources give rise to the traditional idea of the sampling method in electronic measurements (Millman & Taub, 1965), that is, the approach of signal acquisition under a certain successive timing delay between the two pulse sequences having a slight difference in pulse frequencies. The optical analogue of the sampling concept was first introduced to the picosecond pump-and-probe spectroscopic measurement by Elzinga *et al.* (1987) using two separate picosecond lasers. Later the time resolution was markedly improved with the nonlinear optical mixing (NOM) technique for determining the pulse coincidence very accurately (Adachi *et al.*, 1995; Takagi & Adachi, 1999), resulting in the application of this technique to various pump-and-probe measurements of ultrafast dynamics (Adachi *et al.*, 1996, 2000; Takagi & Adachi, 1997). Takagi & Adachi (1999) suggested an extension of the optical sampling to time-resolved measurements in the combined use of laser and synchrotron radiation.

We report an NOM experiment between a self mode-locked laser and the visible output of an optical klystron (OK) inserted into the synchrotron storage ring (Miyamoto *et al.*, 2000). Temporal coincidence was detected as an optical signal of sum-frequency (SF) waves generated in a nonlinear crystal from the two light sources. By setting the laser pulse frequency to be slightly detuned from that of the OK radiation, a burst of

SF signal arising at successively delayed timing around the exact coincidence has been observed. The obtained profile represents a second-order intensity correlation function between the pulses from the two sources (which we denote as cross correlation) and gives substantially an OK pulse profile because the laser pulse is as short as 0.6% of the OK pulse. Although the pulse frequency of our home-built laser fluctuated by more than 10^{-6}, time accuracy within a few picoseconds is readily available by properly choosing the difference in pulse frequencies without any synchronization control. As a result, a narrowing of the OK pulse with decaying bunch current is detected. The energy efficiency in the SF conversion is discussed to confirm the applicability of the present technique in the more conventional use of visible synchrotron radiation from bending magnets. Finally, the future prospects of this technique, to be extended toward the femtosecond time domain and higher energy spectral domain, are described.

2. Principle of optical sampling

The cross-correlation function between two pulse sequences with pulse intensities I_1 and I_2 is defined by

$$G(\tau) = \int_{-\infty}^{\infty} I_1(t+\tau) I_2(t)\,\mathrm{d}t. \qquad (1)$$

When a medium for SF generation is irradiated by two pulse sequences with pulse periods of T_1 and T_2, where

$$I_1 \equiv \sum_n I_1(t - mT_1) \quad \text{and} \quad I_2 \equiv \sum_m I_2(t - nT_2) \qquad (2)$$

(m and n are integers), SF waves are generated in proportion to both the pulse intensities. Here, $I_1(t - mT_1)$ and $I_2(t - nT_2)$ are appropriate functions representing pulse waveforms with peaks at $t = mT_1$ and nT_2, respectively. If the detection cannot follow the instantaneous interaction within the pulse duration, as is usual for measurement in the time scale of a picosecond or less, the intensity profile of the SF wave to be observed is given by

$$F(T_1, T_2) = \sum_{m,n=-\infty}^{\infty} \int_{-\infty}^{\infty} I_1(t - mT_1)\, I_2(t - nT_2)\,\mathrm{d}t. \qquad (3)$$

Assuming that the pulse durations are much shorter than T_1 and T_2, the integration time is taken substantially in the interval in which the pulses overlap. Equation (3) is rewritten within a time interval for one sampling sequence around $t = 0$, *i.e.* for $|m - n| < 1$, as

$$\big[F(T_1, T_2)\big]_{\text{seq.}}^{\text{single}} = \sum_n \int_{-\infty}^{\infty} I_1\big[t - nT_2 + n(T_2 - T_1)\big] I_2(t - nT_2)\,\mathrm{d}t, \quad (T_2 > T_1), \qquad (4)$$

where the summation for n applies to the pulses of I_1 and I_2 in the interval of the sampling sequence. Equation (4) represents a cross correlation between $I_1(t)$ and $I_2(t)$, with the variable $n(T_2 - T_1)$ corresponding to τ in equation (1), and the profile is demonstrated as an envelope of the train of pulses at $t = nT_2$. The increment of the delay time in every pulse period, *i.e.* the resolution limit, is $T_2 - T_1 = \Delta/(f_1 f_2)$, where f_1 and f_2 are the pulse frequencies and $\Delta = f_1 - f_2$. The cross correlation is then seen on a profile of the sampling sequence as expanded by a factor of f_1/Δ, that is, the number of pulses in one sampling sequence. A simulation of the cross-correlation profile using equation (3) is shown in Fig. 1.

When one designs a pump-and-probe experiment using the sampling technique, a part of the pump-and-probe beam is separated and fed into the SF-mixing crystal in which the signal of pulse coincidence is produced. This signal plays a triggering role and provides the time origin of the measurement. This signal waveform, seen in the form shown in Fig. 1, can be used by itself for the pulse diagnostics of the light sources. For this purpose Δ should be chosen as $\tau_1 \gg \Delta/(f_1 f_2)$, where τ_1 is the pulse duration in I_1 under test, so that the profile contains a number of spikes sufficient for reproducing the outline of the profile.

3. Experimental setup

The experimental setup for NOM using a combination of laser and synchrotron radiation is shown in Fig. 2. One of the light sources is a home-built self mode-locked Ti:sapphire laser with an average power of 100 mW, a pulse width of 300 fs and a variable pulse frequency of around 83 MHz with a fluctuation in the range ± 100 Hz. The pulse bandwidth is 50 cm^{-1} at a wavelength of 800 nm. The partner synchrotron radiation source is an 83.33 MHz single-pass visible emission from an OK (a couple of undulators and an in-between modulator) (Miyamoto *et al.*, 2001) operating under the equi-interval 33-bunch mode at the 'New SUBARU' electron synchrotron storage ring. The spectrum is shown in Fig. 3. The NOM medium is a single crystal of type-I β-barium borate (BBO) of length 8 mm, cut at 29° from the optical axis (prepared for the

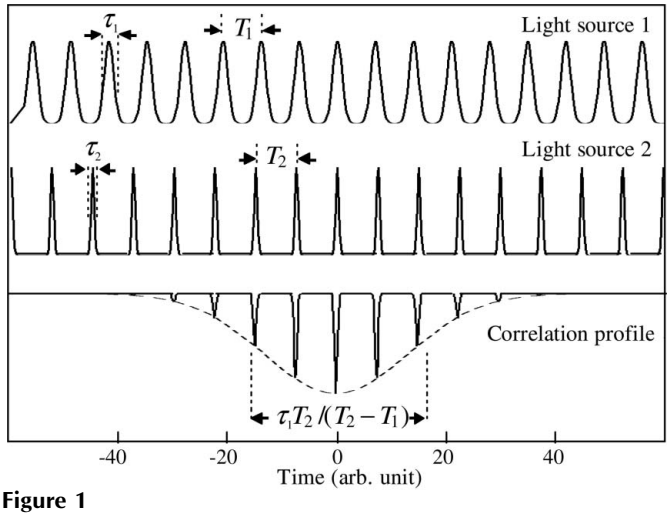

Figure 1
Simulated cross-correlation profile using equation (3), from two Gaussian-pulse sequences with periods of $T_1 = 7$ and $T_2 = 7.5$ and pulse widths of $\tau_1 = 2$ and $\tau_2 = 0.67$. The integration in (3) was omitted because of the large difference in the pulse widths. A dashed curve is shown from the pulse profile of light source 1 with the magnification factor $(T_1\Delta)^{-1} = 14$. Parameters are in arbitrary units. Negative polarity in the profile is chosen intentionally for reference to the experiment.

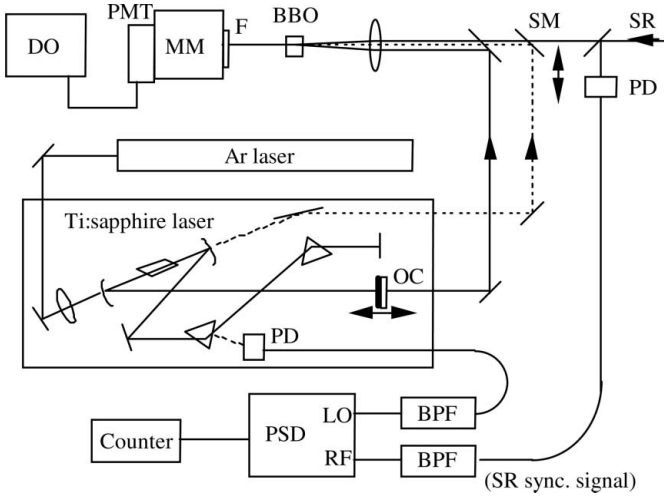

Figure 2
Experimental setup for nonlinear optical mixing using a combination of laser and synchrotron radiation. For a preliminary experiment the output of the Ti:sapphire laser and part of the Ar laser beam (dotted lines), both with an average power of 100 mW, were collinearly focused on the BBO crystal with a 150 mm focal length lens. The Ar laser was then switched to the synchrotron radiation beam with a sliding mirror. The output coupler of the Ti:sapphire laser was mounted on a translation stage to vary the pulse frequency. Mode-locked operation was initiated by shaking the translation stage. Photodiode signals of the pulse trains of the Ti:sapphire laser and synchrotron radiation were mixed to detect the difference in pulse frequencies. When a synchronized RF signal of the synchrotron radiation pulses is supplied it is conveniently used in place of the synchrotron radiation light, though it is not essential for the experiment. DO: digital oscilloscope; PMT: photomultiplier tube; MM: monochromator with 0.5 mm slits; F: filter; SM: sliding mirror; SR: synchrotron radiation; PD: photodiode; OC: output coupler; BPF: band-pass filter; PSD: phase-sensitive detector. The BPFs and PSD are designed for 76 ± 10 MHz.

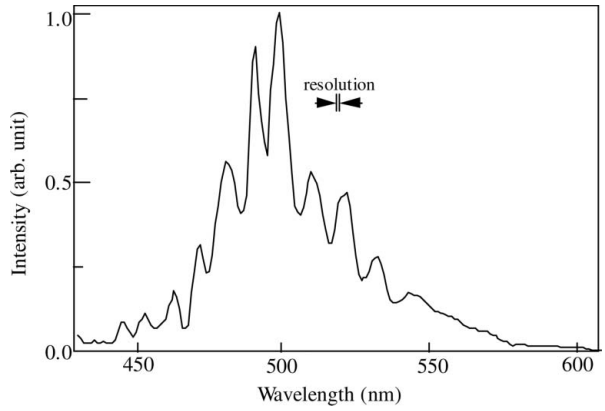

Figure 3
Spectrum of the optical klystron output. The monochromator resolution is 1 nm. The beam current was 0.85 mA bunch^{-1}. The spectrum was measured at the place of optical mixing with the same monochromator as used there. The angle divergence of the output beam is 1.25 mrad in the horizontal plane and 0.5 mrad in the vertical plane. The periodical structure is due to the interference in successive superposition of radiation from the electrons passing through the undulator. The total average power is typically 1 mW.

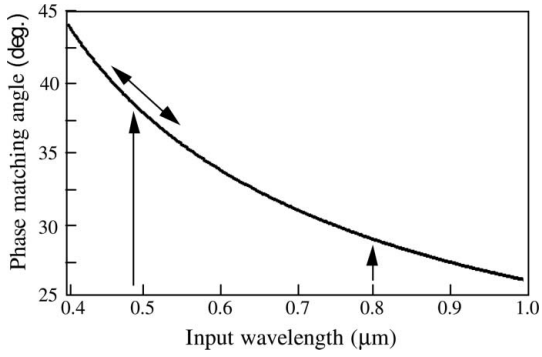

Figure 4
Dependence of the BBO phase-matching angle on the wavelength of one of the input waves for sum-frequency mixing. The wavelength of the other input wave is fixed to 0.8 μm. Vertical arrows at 0.8 and 0.49 μm show, respectively, the second-harmonic generation from the Ti:sapphire laser and sum-frequency mixing with the Ar laser. A double arrow indicates the spectral range in the optical klystron radiation.

type-I phase matching of second-harmonic generation from the 800 nm fundamental).

For a preliminary NOM experiment, a combination of the Ti:sapphire laser and a continuous-wave (cw) argon ion (Ar) laser at 488 nm was used for the following reasons: (1) mixing with a cw light is free from the timing problem, making it easier to find the signal, (2) the phase-matching angle of the nonlinear crystal is close to that for the OK light, and (3) evaluation of the detectability for such a low-power and monochromatic input is useful for estimation of the expected signal intensity for mixing with the OK light. Starting with a search for the second-harmonic generation from the Ti:sapphire laser, which can readily be found by eye, and knowing the current angle of the crystal, we were able to approach the angle for the best SF conversion with the Ar laser and finally with the OK light.

The experiment with the OK light was performed at different bunch currents in the range 0.85–0.4 mA along the natural decay of the bunch current. To detect the difference frequency Δ of the Ti:sapphire and OK pulse trains, a part of their beams was separated and monitored with fast photodiodes, and the signals after band-pass filters around 83 MHz were mixed in a phase-sensitive detector. The value of Δ was read every time the correlation profile data were acquired.

4. Experimental results and discussion

The efficient nonlinear optical conversion stems from the phase matching, *i.e.* the momentum conservation between the input and resultant (sum-frequency) optical waves given by $n_1\omega_1 + n_2\omega_2 = n_3\omega_3$, where n_i and ω_i are refractive indices and angular frequencies of the interacting waves, respectively. For a birefringent crystal to satisfy this condition, a particular propagation angle with respect to the optical axis of the crystal must be chosen according to the characteristics of angle-dependent refractive index. This angle (phase-matching angle) is calculated (Dmitriev *et al.*, 1999), as in Fig. 4, for BBO as a function of the wavelength in one of the incident waves. For detecting the SF signal a monochromator and UV filters were necessary to avoid the background of the fundamental and second-harmonic of the Ti:sapphire laser, which is much stronger than the signal even under large phase-mismatching. For mixing with the Ar laser the quantum conversion effi-

ciency is estimated. The number of input Ar laser photons during the temporal overlap with the 300 fs Ti:sapphire pulse is 3×10^4. The typical SF signal intensity of 20 mV yields the number of photons as 2.5×10^3 per pulse, assuming a response time of 2 ns for a 50 Ω-terminated photomultiplier tube (PMT) and an oscilloscope, a PMT gain of 10^5, a quantum efficiency of 0.2, and one-order-of-magnitude loss by insertion of the monochromator and filters. We obtain a quantum conversion efficiency of roughly 10%, which is likely to be close to the saturation region. By reducing the Ar laser input, the lowest detectable power was found to be 0.45 mW and the signal waveform became foggy, indicating that the signal is as low as in the photon-counting level. From this result we expect the lowest power of the OK pulse train (for a 50 ps pulse duration) to be 2 μW for detection of mixing with the Ti:sapphire laser.

We found the signal of the SF wave at around 306 nm without changing the crystal angle, as expected from the overlapped phase-matching angle for the Ar laser and the OK light (Fig. 4). A typical digital oscilloscope trace of the signal waveform is shown in Fig. 5. The average input power of the OK light giving a signal intensity of ∼20 mV was measured to be 0.2 mW. These values yield a quantum conversion efficiency of roughly 10%. The net input power contributing to the SF generation would be lower than 0.2 mW taking into account the large spectral width in the OK light. We infer that the quantum conversion efficiency within the phase-matching bandwidth reaches the saturation region as in mixing with the Ar laser.

The signal during the sampling sequence of 80 μs would not be affected by noise or fluctuation, as the predominant noise lies in the region $< 10^3$ Hz, originating mainly from mechanical sources. However, averaging the waveforms and reading the value of Δ took several seconds and the results were affected by the fluctuation to some extent. The signal-to-noise ratio was still good enough for the oscilloscope to be triggered internally without causing visible broadening of the waveform or smearing of the spikes during averaging over several tens of sequences. To obtain smoother profiles and higher intensities, the detection bandwidth may be lowered. We have used various termination resistors at the PMT output for this purpose. In order for the detection bandwidth not to affect the correlation trace the detection bandwidth F must be related to the correlation width τ_c, as $\tau_c f_2 F > \Delta$ (Adachi *et al.*, 1995). Because of the limited stability of our laser, Δ fluctuates by ±100 Hz in a few seconds. We have chosen $\Delta \simeq 12$ kHz, so that the fluctuation remains within ±1% error in determining the correct correlation width. We then obtain $F > 3$ MHz. The present measurement satisfies this condition. To derive the parameters of the profile the data points at the peak of the spikes were picked up and made into a simple profile, and then fitted by a Gaussian curve. For Gaussian input pulses with widths of τ_1 and τ_2, their cross-correlation profile gives a width of $\tau' = (\tau_1^2 + \tau_2^2)^{1/2}$. For $\tau_1 = 50$ ps and $\tau_2 = 300$ fs the difference between τ' and τ_1 is only 0.9 fs, so that the observed profile width around 50 ps reproduces substantially the width of the input OK pulse.

The dependence of the measured value of the OK pulse width on the fluctuation in Δ is plotted in Fig. 6. The change in Δ was produced by varying the length of the laser cavity. Large scattering in the values of the pulse width in the region lower than $\Delta \simeq 1$ kHz represents the serious influence of the fluctuation in Δ, because the fluctuation is independent of the value of Δ. An allowable range of fluctuation in Δ can be defined in terms of a deviation from the correct value of the pulse width (assumed to be 52 ps) that coincides with the time resolution $\Delta/(f_1 f_2)$, *i.e.* a time-resolution-limited error. The curve shown in Fig. 6 indicates this range of fluctuation in Δ as a function of Δ. For the area above this curve the accuracy of the pulse width is determined by the fluctuation in Δ, and below the curve the accuracy is limited by the time resolution.

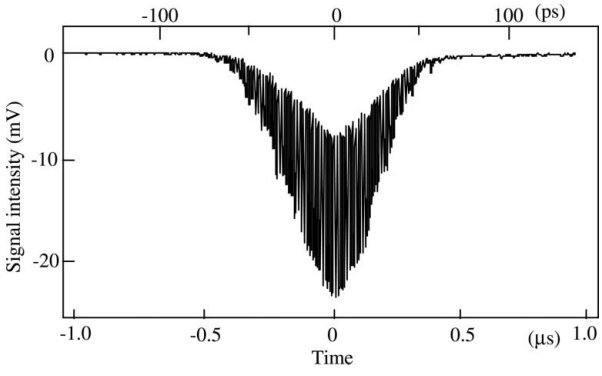

Figure 5
Averaged oscilloscope trace of the cross-correlation profile between the Ti:sapphire laser and the optical klystron radiation. The pulse-frequency difference is $\Delta = 12\,300$ Hz and the increment of delay is $\Delta/(f_1 f_2) = 1.79$ ps. One sampling sequence completes in $\Delta^{-1} = 80$ μs. The upper time scale, as an equivalent time, is obtained from the lower time scale after division by f_1/Δ. The PMT was terminated with 50 Ω impedance, giving a bandwidth of $F \geq 100$ MHz. Repetitive spikes correspond to the Ti:sapphire pulse train. The slightly rugged envelope on the trace even after averaging is a result of the limited sampling rate of the oscilloscope for this sweep time range.

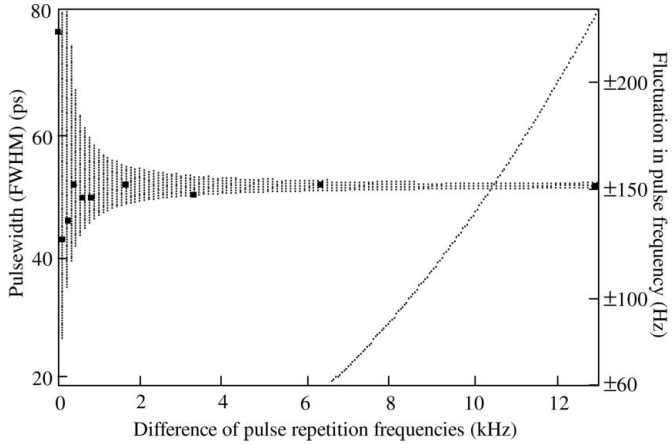

Figure 6
Dependence of the measured optical klystron pulse width on the difference in pulse frequencies Δ. The shaded area indicates the range of pulse-width fluctuation expected from the fluctuation in Δ by ±100 Hz. The curve shows fluctuations in Δ giving the error in the pulse width of the optical klystron radiation, which coincides with the time resolution $\Delta/(f_1 f_2)$.

From this curve we find that for our case of a fluctuation of ± 100 Hz the optimum value of Δ is expected to be 8.5 kHz and the error in the pulse width is $\Delta/(f_1 f_2) = 1.2$ ps.

Fig. 7 shows the dependence of the pulse width of the OK light on the electron bunch current, measured for a period of 5 h along the natural decay of the bunch current. The range of scattering in the data is 2–3 ps. The fluctuation in Δ by ± 100 Hz at $\Delta \simeq 12$ kHz should lead to an error range of $\pm 1\%$ (± 0.5 ps). Scattering in the data is likely to originate from the time-resolution-limited error, $\Delta/(f_1 f_2) = 1.8$ ps, discussed above. Therefore, a higher accuracy would have been attained even for the ± 100 Hz fluctuation if we had chosen the optimum value of $\Delta \simeq 8.5$ kHz. However, it is more requisite to improve the stability in the pulse frequency of the laser, for example, reduction of the mechanical vibration and air turbulence. Nevertheless, the data in Fig. 7 demonstrate a discernible dependence of the pulse width on the bunch current in the measured range. The values and the rate of decrease (-14.5 ps mA^{-1}) in the pulse width along the decay of the bunch current are well in accordance with the lower edge of the bunch-current dependence of the pulse width measured by a picosecond streak camera in relatively higher bunch currents (Ando *et al.*, 2004).

5. Estimation of efficiency in sum-frequency conversion

The efficiency in SF conversion from the OK light should be confirmed because the signal in the present technique, giving the pulse coincidence from the two light sources, serves not only the synchrotron radiation pulse diagnostics but also the timing signal of various pump-and-probe measurements. A higher sensitivity would be required in most measurements using synchrotron radiation from bending magnets with much lower spectral power density than the OK output. According to the theory of three-wave interaction in nonlinear media

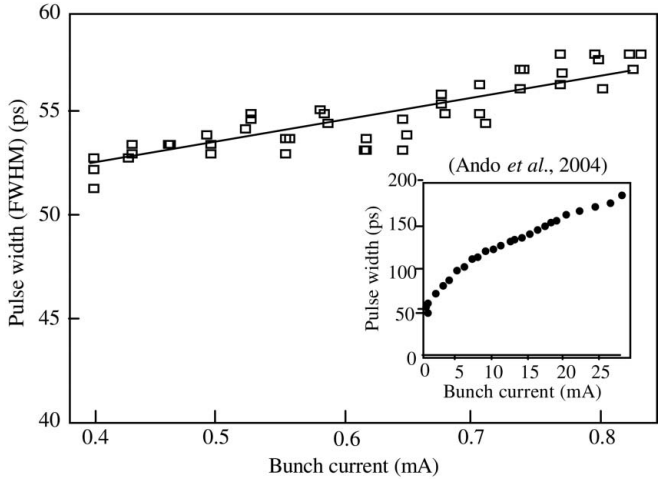

Figure 7
Dependence of the pulse width of the optical klystron radiation on the storage-ring electron bunch current. Δ was read in the range 12100–12400 Hz according to the long-term drift. The solid line shows a least-squares fit (14.5 ps mA^{-1}) for the slope. The pulse width measured by a picosecond streak camera in a relatively higher bunch-current region is shown in the inset for reference.

Table 1
Parameters of equation (5).

P_2 (kW)	n_i	A (mm^2)	$d_{\rm eff}$ (mV)	z (mm)	Wavelength wave1, wave2 (nm)
4	1.6	0.01	1.8×10^{-12}	8	500, 300

(Shen, 1984) a couple of input waves (denoted as wave 1 and wave 2) create an SF wave (wave 3) by second-order nonlinear polarization in a medium. The ratio of the photon flux of wave 3 to that of wave 1 at the interaction length z under a much more powerful wave 2 (so that the photon consumption for wave 2 can be neglected) is given by

$$\frac{P_3(z)\omega_1}{P_1(0)\omega_3} = \sin^2\left[d_{\rm eff} z \left(\frac{2P_2\omega_1\omega_3}{\varepsilon_0 c^3 n_1 n_2 n_3 A}\right)^{1/2}\right], \qquad (5)$$

where P_i are peak powers of the interacting waves, $d_{\rm eff}$ is the effective nonlinear coefficient, ε_0 is the vacuum dielectric constant, c is the velocity of light and A is the beam cross section of the interacting area. Equation (5) expresses an oscillatory energy transfer between wave 1 and wave 3 along the propagation distance. Taking the values listed in Table 1 for our case we get $P_3(z)\omega_1/P_1(0)\omega_3 = \sin^2(0.72\pi)$. This indicates that the quantum conversion efficiency is under the saturation regime where the energy depletion in wave 1 is significant, although (5) holds for the restricted condition of exact phase matching and plane wave interaction, and the conversion efficiency should be reduced to some degree. Consequently the estimation from the theoretical formula supports the experimental result that the conversion efficiency is of the order of 10%.

In the case that the input of the SF conversion is a combination of spectrally wide waves, a spectrally acceptable range for the phase matching must be considered. On the basis of the nonlinear equations describing the three-wave interaction, the energy conversion efficiency obeys the wave mismatch as $\sin^2(|\Delta k|L/2)/(|\Delta k|L/2)^2$ (Shen, 1984), where $\Delta k \equiv k_1 + k_2 - k_3 = (n_1\omega_1 + n_2\omega_2 - n_3\omega_3)/c$ and L is the crystal length. The value of Δk at which the conversion efficiency is halved at the exit of the crystal is then given by $|\Delta k| = 0.886\pi/L$. The corresponding spectral bandwidths $\Delta\omega_1$ and $\Delta\omega_2$ for the input waves are related to Δk by

$$|\Delta k| = \left|\sum_{i=1}^{2} \frac{\partial(\Delta k)}{\partial\omega_i}\Delta\omega_i\right| \qquad (6)$$

and

$$\frac{\partial(\Delta k)}{\partial\omega_i} = \frac{1}{c}\left[n_i - n_3^{\rm e}(\theta) - \lambda_i\frac{\partial n_i}{\partial\lambda_i} + \lambda_3\frac{\partial n_3^{\rm e}(\theta)}{\partial\lambda_3}\right],$$

where λ_1, λ_2 and λ_3 are, respectively, the wavelengths of the synchrotron radiation, the laser and the SF waves. $n_3^{\rm e}(\theta)$ is the refraction index for an extraordinary ray propagating at the phase-matching angle θ ($= 37^\circ$). Substituting into (6) the above value for Δk and $\Delta\omega_2/(2\pi) = 50$ cm^{-1} for the laser, and using the dispersion equations of the refraction indices

(Dmitriev *et al.*, 1999), the accepted bandwidth is given by $\Delta\omega_1 = 63\ \mathrm{cm}^{-1}$. Therefore, the accepted spectral width is determined by the laser-pulse bandwidth. This value is smaller than the width of the interference fringe in the spectrum of the OK light seen in Fig. 3 ($\sim$400 cm^{-1}), and indeed the SF signal intensity oscillated when the mixing crystal was rotated (keeping the monochromator following the phase-matching wavelength).

The number of photons contained in the bending-magnet synchrotron radiation beam from the 'New SUBARU' is 10^3 per pulse within the spectral width of 10 cm^{-1} at a wavelength of 500 nm. Taking into account temporal overlap with the 300 fs laser pulse and 60 cm^{-1} phase-matching bandwidth, the effective number of photons is expected to be 10^1–10^2, which is two to three orders of magnitude lower than the OK pulse. The detection sensitivity for SF generation should therefore be as high as the photon-counting level. The present work shows a cross-correlation profile with a signal-to-noise ratio as high as 10^2; in addition, the detectability can be improved by reducing the detection bandwidth at lower pulse-frequency differences under more stabilized laser conditions. Consequently, the signal, at least under repetitive sampling and averaging, could be detected for bending-magnet synchrotron radiation. This experiment is currently being undertaken.

6. Toward femtosecond resolution

As far as synchrotron radiation pulses of picosecond or subpicosecond time scales are concerned, the direct means for time-resolved measurements would be the use of a streak camera. The sampling technique is more significant in the ultrashort time domain which is not accessible by a conventional streak camera. The measurement time scale is expanded equivalently by a factor of f_1/Δ and the limit of time resolution is given by $\Delta/(f_1 f_2)$, which reaches, for instance, 16 fs for $f_1, f_2 \simeq 80$ MHz and $\Delta = 100$ Hz. If the laser has a pulse width greater than 16 fs the synchrotron radiation pulse diagnostics can be carried out with laser-pulse-limited time resolution. Δ is a key parameter dominating the temporal characteristics of this technique because it determines the equivalent time. If we allow a fluctuation in laser-pulse frequency, for example by 2–3 Hz, the sampling technique gives a time accuracy of 2–3% for $\Delta = 100$ Hz, irrespective of the measurement time scale. Such a range of fluctuation is within the specification of commercially well established lasers. A higher stability in Δ, if necessary, is achievable primarily by optimization of the laser alignment, including the removal of mechanical and thermal instability, and secondly by electronically locking the frequency $f_2 + \Delta$ to f_1. A stable audio-frequency reference signal is mixed with the error signal for Δ by a phase-sensitive detector in the negative feedback loop (Adachi *et al.*, 1995). From our experience Δ can be stabilized within ± 1 Hz in 1 min for a home-built mode-locked laser, giving rise to a time base error of $\pm 1\%$ for $\Delta = 100$ Hz. If one were alternatively to require the accuracy of the same time scale by the exact synchronization of the laser to the synchrotron radiation pulses, the laser cavity length would have to be stabilized within 1 nm fluctuation (Spence *et al.*, 1993).

7. Outlook on the optical sampling technique in different spectral domains

The sampling technique demands detection of the signal for the accurate pulse coincidence between the light sources instead of attainment of strict pulse synchronization. Any physical process originating from correlative interaction between two lights through a material can be a candidate for exhibiting the coincidence of the two lights only if it is an inertia-less process, to maintain explicit simultaneity. We should here confine such processes to those in the UV and X-ray regions, where the nonlinear crystal plays no role. Suitable candidates for nonlinear processes in the UV region are two-photon absorption (Mitsuke *et al.*, 2000) and the two-photon photoelectric effect (Takagi, 1994). For the latter, a number of UV photons in a wide spectral range could contribute to the interaction, but the following condition must be considered: the total photon energy must exceed the work function, and the background of single-photon and multiple-photon processes for the synchrotron radiation and laser alone, respectively, must be suppressed below the level required for extracting the coincidence signal. If energy-resolved detection is available, a portion of the photoelectron energy originating from the process concerned can be extracted for the coincidence. For X-ray experiments using light sources from an insertion device, visible light may not be supplied, so that the coincidence signal must be taken from some correlating interaction between the synchrotron radiation X-ray and laser. Such processes may be categorized as either the synchrotron radiation probing of laser-induced effects or the laser probing of synchrotron-radiation-initiated processes. Of particular interest for the former are the change in X-ray Bragg diffraction due to a laser-induced lattice displacement in organic crystals (Techert *et al.*, 2001), strain in semiconductors (Larsson, 2001), and X-ray fluorescence enhancement in laser-excited semiconductors (Adams *et al.*, 2002). These processes represent the full time course of the interaction around 10^{-10}–10^{-11} s and need a laser fluence of $\sim 10^{-4}$ J cm^{-2}, which is within the range of available levels for high-frequency optical sampling. One of the candidates in the second category would be the laser sensing (absorption, reflection or photoemission) of a variety of low-energy secondary processes for the valence electrons originating from the inner-shell electron excitation and relaxation that terminates extremely quickly. However, the use of these processes would be energetically disadvantageous compared with the first category, since the high-energy photon is used for excitation and the low-energy photon is detected.

Searching the physical processes to show the correlation between the X-ray and laser pulses is by itself a study of ultrafast dynamics in radiation-excited materials as well as the development of ultrafast X-ray detectors. Advances in finding the best devices can be made *via* such studies, especially given

the background of the recent advent of the femtosecond X-ray free-electron laser (Adams, 2003).

8. Summary

An optical sampling method has been applied to a time-correlated measurement for the combined use of ultrashort laser and synchrotron radiation pulses. A cross-correlation profile based on sum-frequency optical mixing provided the profile of a picosecond synchrotron light pulse without employing the mechanism for pulse synchronization. It has been proved that the sampling method allows picosecond pulse diagnostics of synchrotron radiation in combination with a high-repetition-rate ultrashort pulsed laser, even under somewhat poor stability in the pulse frequency. We believe this technique to be successful in the femtosecond time domain using a diagnosing laser with a shorter pulse and higher pulse-repetition stability.

The authors acknowledge useful discussions with A. Ando and Y. Shoji on the pulse characteristics of the optical klystron. This work was partly supported by a Grant-in-Aid for Scientific Research from Hyogo prefecture.

References

Adachi, S., Takagi, Y., Takeda, J. & Nelson, K. A. (2000). *Opt. Commun.* **174**, 291–298.
Adachi, S., Takeyama, S. & Takagi, Y. (1995). *Opt. Commun.* **117**, 71–77.
Adachi, S., Takeyama, S., Takagi, Y., Tackeuchi, A. & Muto, S. (1996). *Appl. Phys. Lett.* **68**, 964–966.
Adams, B. W. (2003). *Nonlinear Optics, Quantum Optics, and UltraFast Phenomena with X-rays.* Boston: Kluwer Academic.
Adams, B. W., DeCamp, M. F., Dufresne, E. M. & Reis, D. A. (2002). *Rev. Sci. Instrum.* **73**, 4150–4156.
Ando, A., Hashimoto, S. & Shoji, Y. (2004). *Proceedings of the Eighth International Conference on Synchrotron Radiation Instrumentation, American Institute of Physics Conference Proceedings 705*, pp. 13–16. Melville, NY: AIP.
Dmitriev, V. G., Gurzadyan, G. G. & Nikogosyan, D. N. (1999). *Handbook of Nonlinear Optical Crystals.* Berlin: Springer.
Elzinga, P. A., Kneisler, R. J., Lytle, F. E., Jiang, Y., King, G. B. & Laurendeau, N. M. (1987). *Appl. Opt.* **26**, 4303–4309.
Gatzke, J., Bellmann, R., Hertel, I., Wedowski, M., Godehusen, K., Zimmermann, P., Dohrmann, T., Borne, A. v. d. & Sonntag, B. (1995). *Nucl. Instrum. Methods Phys. Res. Sect. A*, **365**, 603–606.
Gatzke, J., Winter, B., Quast, T. & Hertel, I. (1998). *Proc. SPIE*, **3464**, 14–19.
Lacoursiere, J., Meyer, M., Nahon, L., Morin, P. & Lazilliere, M. (1994). *Nucl. Instrum. Methods Phys. Res. Sect. A*, **351**, 545–553.
Larsson, J. (2001). *Meas. Sci. Technol.* **12**, 1835–1840.
Meyer, M., Muller, B., Nunnemann, A., Prescher, Th., Raven, E. v., Richter, M., Schmidt, M., Sonntag, B. & Zimmermann, P. (1987). *Phys. Rev. Lett.* **59**, 2963–2966.
Millman, J. H. & Taub, H. (1965). *Pulse, Digital and Switching Waveforms.* Tokyo: McGraw-Hill Kogakusha.
Mitani, T., Okamoto, H., Takagi, Y., Watanabe, M. & Fukui, K. (1989). *Rev. Sci. Instrum.* **60**, 1569–1572.
Mitsuke, K., Hikosaka, Y. & Iwasaki, K. (2000). *J. Phys. B*, **33**, 391–405.
Miyamoto, S., Inoue, T., Amano, S., Fukugaki, K., Shimoura, A., Hashimoto, S., Shoji, Y., Yatsuzuka, M., Ando, A. & Mochizuki, T. (2001). *Proceedings of the 13th International Conference on High-Power Particle Beams*, edited by K. Yatsui & W. Jiang, pp. 230–235. Nagaoka: Nagaoka University of Technology.
Rulliere, C. (2003). Editor. *Femtosecond Laser Pulses.* New York: Springer.
Shen, Y. R. (1984). *The Principles of Nonlinear Optics.* New York: Wiley-Interscience.
Spence, D. E., Sleat, W. E., Evans, J. M. & Sibett, W. (1993). *Opt. Commun.* **174**, 291–298.
Takagi, Y. (1994). *Appl. Opt.* **33**, 6328–6332.
Takagi, Y. & Adachi, S. (1997). *J. Lumin.* **72–74**, 546–547.
Takagi, Y. & Adachi, S. (1999). *Rev. Sci. Instrum.* **70**, 2218–2224.
Tanaka, Y., Hara, T., Kitamura, H. & Ishikawa, T. (2000). *Rev. Sci. Instrum.* **71**, 1268–1274.
Techert, S., Schotte, F. & Wulff, M. (2001). *Phys. Rev. Lett.* **86**, 2030–2033.
Wille, K. (1991). *Rep. Prog. Phys.* **54**, 1005–1067.
Winter, B., Gatzke, J., Quast, T., Will, I., Wick, M. T., Liero, A., Pop, D. & Hertel, I. V. (1998). *Proc. SPIE*, **3451**, 62–69.